

REPORT DOCUMENTATION PAGE					Form Approved OMB No. 0704-0188	
The public reporting burden for this collection of information is estimated to average 1 hour per response, including the time for reviewing instructions, searching existing data sources, gathering and maintaining the data needed, and completing and reviewing the collection of information. Send comments regarding this burden estimate or any other aspect of this collection of information, including suggestions for reducing the burden, to Department of Defense, Washington Headquarters Services, Directorate for Information Operations and Reports (0704-0188), 1215 Jefferson Davis Highway, Suite 1204, Arlington, VA 22202-4302. Respondents should be aware that notwithstanding any other provision of law, no person shall be subject to any penalty for failing to comply with a collection of information if it does not display a currently valid OMB control number.						
1. REPORT DATE (DD-MM-YYYY) 23-07-2003		2. REPORT TYPE REPRINT			3. DATES COVERED (From - To)	
4. TITLE AND SUBTITLE Ion Beam Neutralization Processes for Electric Micropropulsion Applications				5a. CONTRACT NUMBER		
				5b. GRANT NUMBER		
				5c. PROGRAM ELEMENT NUMBER 621010F		
				5d. PROJECT NUMBER 1010		
6. AUTHOR(S) Adrian Wheelock David L. Cooke Nicholas A. Gatsonis*				5e. TASK NUMBER RS		
				5f. WORK UNIT NUMBER A1		
7. PERFORMING ORGANIZATION NAME(S) AND ADDRESS(ES) Air Force Research Laboratory/VSBXR 29 Randolph Road Hanscom AFB, MA 01731-3010				8. PERFORMING ORGANIZATION REPORT NUMBER AFRL-VS-HA-TR-2004-1176		
9. SPONSORING/MONITORING AGENCY NAME(S) AND ADDRESS(ES)				10. SPONSOR/MONITOR'S ACRONYM(S)		
				11. SPONSOR/MONITOR'S REPORT NUMBER(S)		
12. DISTRIBUTION/AVAILABILITY STATEMENT Approved for public release; distribution unlimited.						
13. SUPPLEMENTARY NOTES Reprinted from: Proceedings, 39th AIAA/ASME/SAE/ASEE Joint Propulsion Conference & Exhibit, July 20-23, 2003, Huntsville, AL *Mechanical Engineering Dept., Worcester Polytechnic Institute, Worcester, MA 01609						
14. ABSTRACT While it is common knowledge that ion beams are easily neutralized using a variety of means, the precise process of neutralization remains unknown. With the increasing popularity of electric propulsion, and in particular micropropulsion systems, this question is of significant importance. Additionally, it has a bearing on thruster design, space instrument calibration, electrodynamic tethers, and ionospheric research. A review of the present state of knowledge on this topic is presented as well as results from ion beam simulations using 2D and 3D Particle-in-Cell codes. The grid generation methodology, adaptation, charged-particle transport, and field solver methodologies of the 3D code are reviewed. The simulations show electrons moving to neutralize the ion beam from background and neutralizer sources. The simulations show the dependence of neutralization on beam energy and the electron/ion velocity ratio. The results are compared favorably with previous computations and experimental observations						
15. SUBJECT TERMS Electric propulsion Neutralization of ion beams Plasma simulation						
16. SECURITY CLASSIFICATION OF:			17. LIMITATION OF ABSTRACT		18. NUMBER OF PAGES	
a. REPORT UNCL	b. ABSTRACT UNCL	c. THIS PAGE UNCL	UNL		19a. NAME OF RESPONSIBLE PERSON David L. Cooke	
					19b. TELEPHONE NUMBER (Include area code) (781) 377-2931	

39th AIAA/ASME/SAE/ASEE Joint Propulsion Conference &
Exhibit July 20-23, 2003 Huntsville, AL

AIAA-2003-5148

ION BEAM NEUTRALIZATION PROCESSES FOR ELECTRIC MICROPROPULSION APPLICATIONS

Adrian Wheelock* and David L. Cooke†
Air Force Research Laboratory, Space Vehicles Directorate, Hanscom AFB, MA

Nikolaos A. Gatsonis‡
Mechanical Engineering Department, Worcester Polytechnic Institute, Worcester, MA 01609

Abstract

While it is common knowledge that ion beams are easily neutralized using a variety of means, the precise process of neutralization remains unknown. With the increasing popularity of electric propulsion, and in particular micropropulsion systems, this question is of significant importance. Additionally, it has bearing on thruster design, space instrument calibration, electrodynamic tethers, and ionospheric research. A review of the present state of knowledge on this topic is presented as well as results from ion beam simulations using 2D and 3D Particle-in-Cell codes. The grid generation methodology, adaptation, charged-particle transport, and field solver methodologies of the 3D code are reviewed. The simulations show electrons moving to neutralize the ion beam from background and neutralizer sources. The simulations show the dependence of neutralization on beam energy and the electron/ion velocity ratio. The results are compared favorably with previous computations and experimental observations.

INTRODUCTION

It is well known that electrons injected into an ion beam can readily neutralize it. The method by which the electrons are entrained and remain in the ion beam to neutralize the space charge, however, remains uncertain. Proper modeling of the current coupling and neutralization phenomena will enable development of low-current neutralizers, optimization of neutralizers for electric propulsion devices as well as aid in the development of emerging micropropulsion devices.

In the early years of electric propulsion research, the neutralization question was one of the fundamental issues for successful development of this promising technology. A dense ion beam requires space charge neutralization to avoid a potential barrier that can divert or reflect the beam. The vehicle on which the thruster operates needs current neutrality to avoid excessive charging. In the context of collisionless plasma theory, achieving both current and charge neutrality with the same source of electrons appears to be nearly impossible owing mostly to the large difference in mass between electrons and the ions. For example, define the ion

flux, $F_i = N_i v_i$, and the net electron flux,

$F_e = \sum N_e v_{eth}$, where N is density, v is velocity, i and e are ion and electron subscripts and eth designates the electron thermal velocity for an idealized electron source. Equal density and flux requires $v_{eth} = 4v_i$. A

1 keV Xenon beam has $v_i = 38,000$ m/s so a matching electron velocity requires a source temperature of about 0.05 eV. A challenging, but not impossible number, but a collisionless analysis suggests that detailed balancing is required, whereas real systems quite easily achieve 'beam coupling.' Of course a higher temperature, lower density electron source will lead to a positive potential well that does trap electrons, but then the theory must explain by what process the trapped electrons shed energy so as to actually fill the well. Another observation is that when ion beams and neutralizers are operated in conducting vacuum tanks, the currents are closely coupled even though the grounding tank eliminates the charge accumulation that could provide feedback for current balance so it appears that one or more plasma mechanisms must be responsible for this collective phenomena -- charge and current neutrality -- which we hereafter call beam coupling.

Although the propensity for beam coupling is clearly serendipity for the application of electric thrusters, our review of the literature indicates it is still a conundrum for plasma science. Further, new electric micropropulsion devices such as the FEEP or the colloidal thrusters or large arrays of ion and Hall

* Aerospace Engineer, Ph.D. candidate WPI,
Student Member AIAA

† Research Scientist, Senior Member AIAA

‡ Associate Professor, Senior Member AIAA

This paper is not subject to U.S. copyrights.

Published 2003 by American Institute of Aeronautics
and Astronautics.

20050412 009

thrusters are still not guaranteed to behave. We might also desire a means to predict and optimize neutralizer operations. Thus, a simulation technique exhibiting beam coupling is needed. Additionally, results from ion beam neutralization modeling will be applicable to ion beams for instrument calibration, electrodynamic tethers, ionospheric research, and fundamental plasma physics.

Our immediate goal is to determine if what might be considered standard Particle-In-Cell, PIC, techniques are adequate or if additional treatment is needed to understand and capture the beam coupling process. In this paper we present first a comprehensive review of neutralization studies. We then present a series of simulations using a 2-D PIC code^{1,2,3} as well as the implementation of a 3D PIC/DSMC code.^{4,5} These show the dependence of the beam neutralization on beam energy and neutralization current. The simulations presented in this paper serve also as means of validation of the PIC-modules of our PIC/DSMC code under development.

HISTORY OF EP NEUTRALIZATION

Possibly first pointed out by L. Spitzer in 1952 [uncited note in Seitz et al. 1961], electric propulsion plumes needed to be properly mixed with electrons or else severe space-charge effects would result. Before the first space tests, there were serious doubts as to the stability of any neutralization approach to the ion beam created by an electrostatic thruster. The general idea was for neutralization to occur shortly after emission to prevent beam return. However, there was lack of understanding as to how the electrons would stay within the beam if they were injected or if the neutralization process was unstable to small perturbations. Failing to properly neutralize the beam would cause a dramatic reduction in thrust, as a significant portion of the beam would return to the spacecraft. This problem was first addressed by the Ramo-Wooldridge staff in their review of electrostatic propulsion in 1960.⁶ Their one-dimensional investigation was admittedly unrealistic enough to provide a satisfactory indication as to the stability and practicality of neutralization.

Looking at simplified versions of the problem, many theorists predicted growing instabilities that could turn the beam back to the spacecraft. Seitz et al.⁷ also reviewed the process in 1961, noting that, if electrons were left to drift into the exhaust beam from a stationary start outside of it, the center of the beam would still develop a virtual cathode and suffer from thrust reduction. On the other hand, they found that electrons could likely oscillate within the beam. At the same time, Baldwin⁸ pointed out the necessity of trapping electrons in a potential well created by the

ion beam and French⁹ found that oscillations in electron current density aided in neutralization. Pearlstein et al. (1963)¹⁰ argued that there would exist a possible problem if the neutralizer could only emit in a space-charge limited regime rather than an emission-limited regime. Mirels (1961)¹¹ argued that the location of emitter and thermal motion of electrons would not significantly impact beam neutralization, subject to more general design constraints. Buneman and Kooyers¹², using a one-dimensional PIC code in 1963 were able to provide a neutralized beam when electrons were injected at velocities lower than the directed ion velocity. Fluctuations in the space charge field provided mixing of the beam. Two years later Wadhwa et al.¹³ performed a two-dimensional PIC simulation showing that electrons would oscillate within the beam to allow for neutralization, but theorized that oscillations was not the only mechanism at work. One method suggested was that fluctuations in the space-charge field allowed for entropy increase to mix the electrons, but these fluctuations were not found downstream of the neutralizer.

The 1964 Space Electric Rocket Test I (SERT I) found that it was quite easy to neutralize ion beams in space from a simple neutralizer geometry. In a series of tests it was shown that the ion thruster developed thrust at a level indicating complete beam neutralization even with the neutralizing filament biased significantly from the spacecraft ground.¹⁴ In 1970, SERT II was launched with the objective of demonstrating long-term ion thruster operation. While it quickly developed shorts in both thrusters, these were resolved by 1979 and one of the thrusters was returned to operation. In reference to our discussion, there were two items of note: The neutralizer current and beam current were nearly impossible to decouple and a neutralizer one meter away from the beam was able to neutralize the ion beam indicating that neutralization is easier than previously thought.

After SERT I, proof of concept was achieved and the theoretical discussion of beam neutralization was dropped in favor of engineering new thrusters. Studies after SERT I include evaluations of neutralizer placement^{15,16}, optimization of the thrusters, and simulations to analyze spacecraft-plume interactions.^{17,18} Othmer et al.^{19,20} has investigated the neutralization process using a relativistic 3D PIC simulation to model neutralization of particles moving at around 0.1c, some three to four orders of magnitude higher than typical velocities. The ratio between electron and ion speeds was kept realistic, however. Their findings included a shock front moving through the beam and a sheath near the neutralizer injection area to accelerate the electrons

into the beam. Also, a strong dependence on the ratio of electron thermal velocity and bulk ion speed was observed in two radically different modes of neutralization. The relativistic PIC code, as well as a somewhat unphysical geometry employed, are fundamental shortcomings of the approach. Tajmar and Wang¹⁵ investigated FEEP neutralization. They found that the placement of the neutralizer had significant impact on the potential distribution of the beam. Further numerical studies by Tajmar and Wang¹⁶ investigated backflow contamination and charge exchange effects. Neither work performed a rigorous study of the electron capture process and electron motion within the beam. Similar to FEEPs are Colloid thrusters. These have not been developed as far and no studies of colloid neutralization simulations exist, to the knowledge of the authors.

Additional flight data was achieved with the Deep Space 1 spacecraft, which recorded over 16,000 hours of use of its NSTAR Ion Engine²¹. Due to the fact that electrostatic propulsion was a proven concept, less interest was paid to neutralization and most numerical studies supporting the mission focused on contamination and sputtering issues²¹ and in fact there was no instrumentation to measure the beam-neutralizer coupling.²² Wang et al.¹⁸ used a PIC code where only charge-exchange particles were modeled as particles and electrons were set to a Boltzmann distribution with density to neutralize the beam appropriately. In-flight data collection focused on charge-exchange plasma characterization.²³

Additionally, ion beam release studies performed as part of the PORCUPINE project²⁴ suggested that electrons within the ion beam would leave after a short distance, as they would have too much kinetic energy. This suggests that the ambient plasma may play a greater role than previously assumed, which may change operating parameters and capabilities of electric propulsion devices in different environments.

Despite decades of research and the implementation of electric propulsion devices, the detailed process by which an ionized beam is neutralized in space is still unknown. Assorted methods to fit data with theory have been found, but the actual process has yet to be studied in sufficient detail to fully understand the subject.

UNSTRUCTURED 3D PIC CODE DESCRIPTION

While the majority of our simulations were performed using the code XPDP2^{1,2,3}, we have also begun using our 3D PIC/DSMC code to examine the problem in a more realistic fashion. We have developed an unstructured grid generator that provides three-dimensional meshes of arbitrary

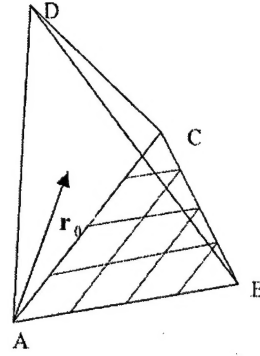


Figure 1: Tetrahedral Cell

geometry and allows for adaptation of the mesh according to the preliminary solution obtained on an initial grid.^{4,5} The generator is based on Watson's²⁵ incremental node insertion method, using properties of Delaunay²⁶ triangulation.

The general procedures for loading and injection used in this work follow Birdsall et al.²⁷ and Bird.²⁸

Integration of the equations of motion of a charged particle are performed by the Boris method²⁹ as discussed by Birdsall et al.²⁷ Particles are moved between adjacent cells using a particle-tracing technique, as shown in Figure 1.

To formulate a finite volume method for Poisson's equation

$$\nabla^2 \Phi = -\frac{\rho}{\epsilon_0} = -\frac{\sum_{i=1}^{N_i} q_i n_i + q_e n_e}{\epsilon_0}, \quad (1)$$

advantage is taken of the Voronoi dual of the Delaunay triangulation to associate an irregular volume to each node on the grid. The Voronoi cell corresponding to each Delaunay node contains the set off points closer to that node than any other, the facets of the Voronoi cell are orthogonal to the lines

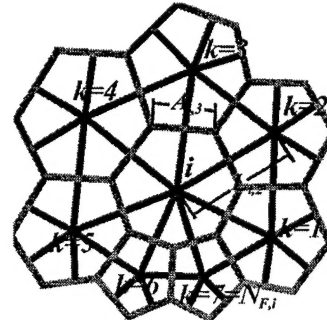


Figure 2: Delaunay-Voronoi Cell

Constant Simulation Parameters					
nc_x	nc_y	L_x	L_y	τ	L_{elec}
128	128	0.05	0.05	2.0E-10	0.025
n_{bg}	W	m_{ion}	E_{ze}	T_i	T_e
1E11	1e4	2.18e-25	0	0.1	0.01
Simulation Variables and Results					
Case	j_i	j_e/j_i	E_{zi}	ϕ_{max}	P
1.1	7.67E+18	1.00	40	67.1024	1.21E-6
1.2	7.67E+18	5.47	40	7.6241	1.21E-6
1.3	1.21E+19	1.00	100	111.8380	4.85E-7
1.4	1.21E+19	3.46	100	1.7708	4.85E-7
1.5	3.83E+19	1.00	1000	20.6984	4.85E-8
1.6	3.83E+19	1.09	1000	1.5144	4.85E-8

Table 1: Simulation Parameters for Simulation Set 1

joining the tetrahedral nodes as shown in Figure 2.

This method reduces Gauss' law for a node-centered finite volume scheme to the standard 2nd order finite-difference method on Cartesian meshes.

In a bounded domain, piece-wise Dirichlet and Neumann boundary conditions specify a solution of Poisson's equation. Since the boundaries of the Delaunay mesh are forced to coincide with the boundaries of the computational domain, boundary condition implementation is straightforward. In the case of a Dirichlet boundary condition, the voltage is placed on the right hand side of the matrix and the corresponding row is zeroed, with a one placed on the diagonal. Fluxes in Neumann boundary conditions are added to the flux formulation for the Voronoi cell corresponding to the boundary node, with the value of the inward normal electric field multiplied by the boundary area added to the right hand side of the node of interest.

In matrix form with boundary conditions as in Figure 3, Gauss' law is:

$$\begin{bmatrix} 1 & 0 & 0 & \dots & 0 \\ R_{2,1} & R_{2,2} & R_{2,3} & \dots & R_{2,N} \\ R_{3,1} & R_{3,2} & R_{3,3} & \dots & R_{3,N} \\ \vdots & \vdots & \vdots & \ddots & \vdots \\ R_{N,1} & R_{N,2} & R_{N,3} & \dots & R_{N,N} \end{bmatrix} \begin{bmatrix} \Phi_1 \\ \Phi_2 \\ \Phi_3 \\ \vdots \\ \Phi_N \end{bmatrix} = \begin{bmatrix} Q_1 \\ Q_2 + \epsilon_0 E_{N,2} A_{N,2} \\ Q_3 \\ \vdots \\ Q_N \end{bmatrix} \quad (2)$$

N is the number of nodes in the mesh. The coefficients are determined by

$$R_{i,j} = \sum_{k=1}^{N_{f,i}} \frac{A_{i,k}}{L_{i,k}} \text{ for } i=j, \quad (3)$$

$$R_{i,j} = -\frac{A_{i,j}}{L_{i,j}} \text{ if } j \text{ is adjacent to } i,$$

$$R_{i,j} = 0 \text{ otherwise.}$$

$\frac{A_{i,j}}{L_{i,j}}$ is the ratio of the area of

the Voronoi face A_{ij} between nodes i and j to the distance between nodes i and j if the nodes L_{ij} . The boundary conditions for node 1 are Dirichlet with potential Φ_0 , and

node 2 is on a Neumann boundary with inward flux $E_{N,2} A_{N,2}$.

SIMULATIONS AND RESULTS

In this section, we present the results of a series of 2D and 3D ion beam simulations. As explicit 3-D simulations are computationally intensive, the

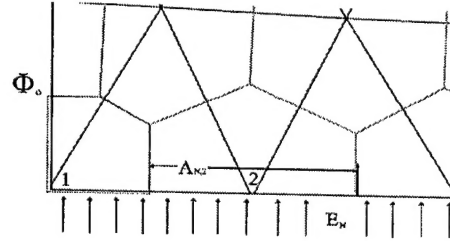


Figure 3: Boundary Conditions in Delaunay-Voronoi Dual.

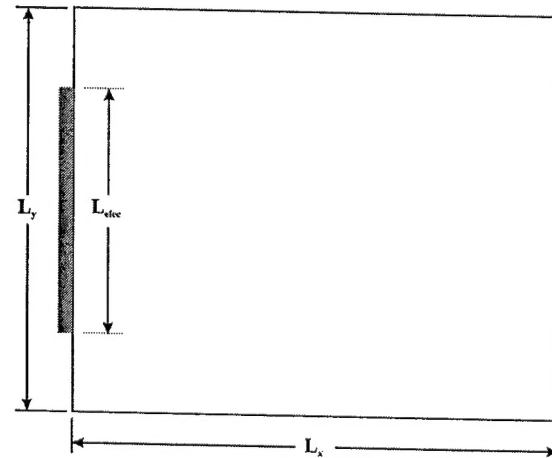


Figure 4: 2-D Simulation Domain

majority of our results have been derived using the 2-D code XPDP2.^{1,2,3}

2-D Results

We performed a variety of simulation runs examining the following parameters: current density j_i and j_e , injection energy E_{x_i} and E_{x_e} , and thermal (random) energy T_i and T_e . The cases run and the selected parameters are listed in Table 1. The parameters are not modeled after any specific system but are intended to be representative of the class of problems associated with electric propulsion.

The simulation domain for the 2-D simulations is shown in Figure 4. A square domain was chosen for simplicity with $L_x = L_y = 0.05$ m. The number of cells along each axis was $nc_x = nc_y = 128$. A single electrode was placed along the left wall with length $L_{elec} = 0.025$ m. A background density of $n_{bg} = 1.0 \times 10^{11} \text{ m}^{-3}$ was selected to compare to LEO operations. The particles were given a

weighting factor of $1E4$ to allow for a uniform background of simulated particles.

Results from the 2-D runs are shown in figures 5 through 11. Figures 5 and 6 show typical $V_x - x$ phase space plots for the ions of a neutralized and a non-neutralized ion beam respectively. Clearly visible is the reflection of a portion of the beam to the emitter in the non-neutralized case. The slight dip in directed velocity as visible in the "neutralized" case is due to a slight potential build-up within the beam that is insufficient to retard the beam to reflection.

First, the dependence on injected electron density was examined at beam energies of 40, 100, and 1000 eV and a plasma density of $1 \times 10^{15} \text{ m}^{-3}$. This resulted in currents in the milliamp range, i.e. for run 1.1 the ion and electron current was matched at $qL_{elec}L_x j = 3.07E-4 \text{ A}$. The electron current was set to match either the ion beam current to simulate current neutralization, or so that the resulting density would match that of the ion beam for density-neutralization. Throughout this series of simulations we kept the electron thermal temperature low, but not

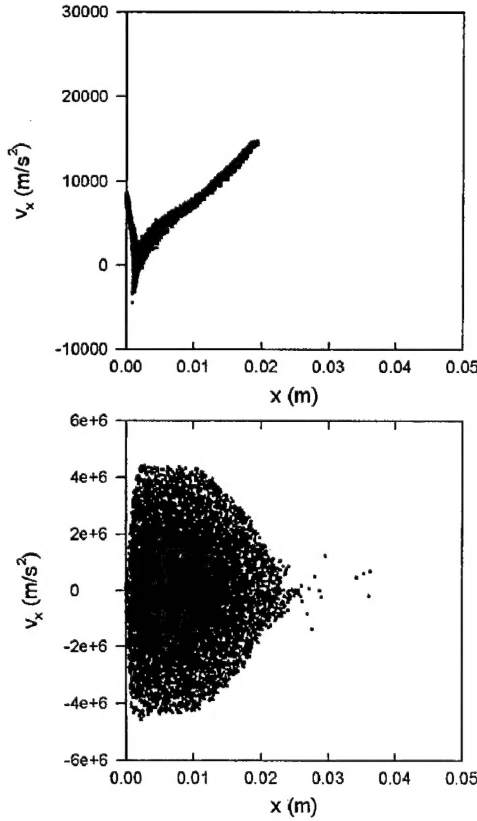


Figure 5: $V_x - x$ phase space for Case 1.1, $\tau = 1.8E-6$ s. Top: ions, Bottom: electrons.

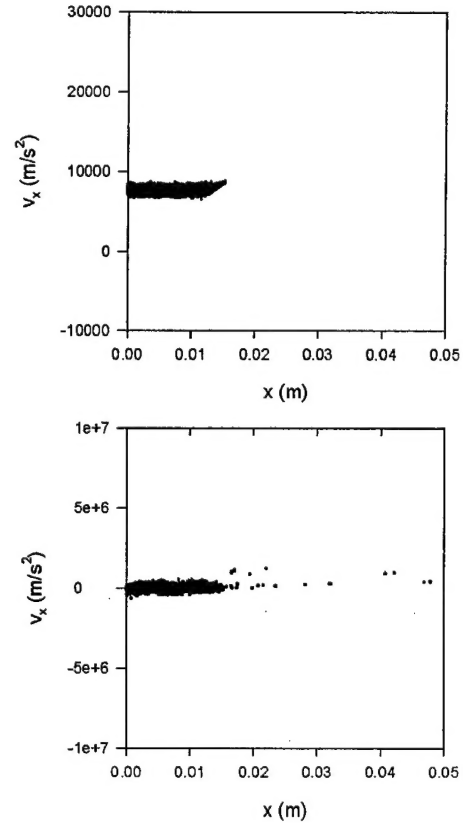


Figure 6: $V_x - x$ phase space for Case 1.2, $\tau = 1.8E-6$ s. Top: ions, Bottom: electrons.

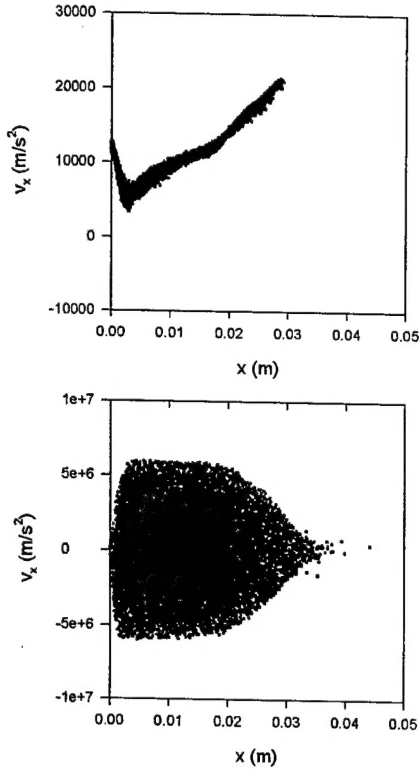


Figure 7: $V_x - x$ phase space for Case 1.3, $\tau=1.8\text{E-}6$ s. Top: ions, bottom: electrons.

zero, as seen in Table 1. Electron directed energy (E_x) was set to zero to simply “place” the electrons on the emission surface.

The current-neutralized beam developed a virtual anode and reflected at 40 and 100 eV energies, but it was neutralized at 1000 eV, showing only a slight potential increase over the background. Phase space plots are shown in Figures 5 through 10. The surprising neutralization at 1000 eV beam energy led to the second simulation set.

The second set of simulations investigated the relation between electron temperature and beam energy. A requirement for low electron velocities is similar to the argument put forth by the Ramo-Wooldridge Staff.⁴ They found, using a one-dimensional model, that the beam would be unstable unless electron speeds were less than ion speeds. A series of simulations was performed to find where, if anywhere, the electron temperature would produce a velocity that would create a neutralized beam, in comparison to cases 1.1 and 1.3, or an unneutralized beam, in comparison to case 1.5. The varied parameters are listed in Table 2, all other parameters are the same as the base case.

Unexpectedly, the 1000eV beam would only develop a virtual cathode when the electron

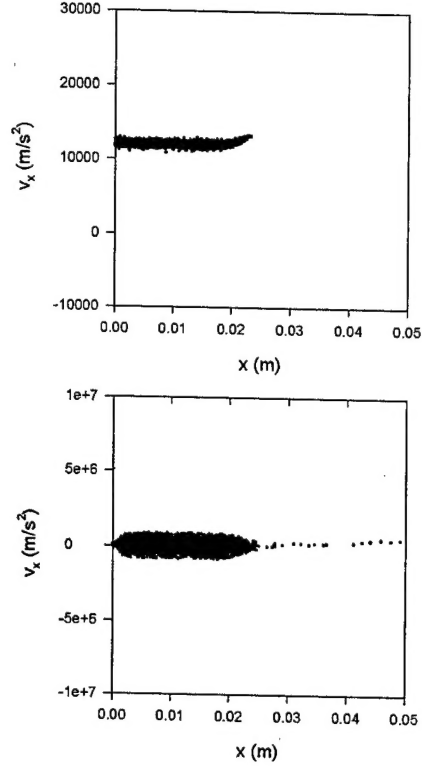


Figure 8: $V_x - x$ phase space for Case 1.4, $\tau=1.8\text{E-}6$ s. Top: ions, bottom: electrons.

temperature was brought to a full eV. This corresponded with an electron/ion speed ratio of nearly 11. The 100eV case could not become successfully neutralized even with an electron/ion speed ratio of 0.5! This dramatically illustrates that electron temperature is not the dominant factor in the neutralization of ion beams.

In all simulations, the circulation of the electrons along the beam lengthwise is observed. The velocities of the circulating electrons are significantly higher if they are unable to neutralize the space charge of the ion beam. There is a slower “core” visible that corresponds with the bulk of the ion beam, visible in the unneutralized simulations. Additionally, one can see a sheath formed on the

Case	Base case	T_e (eV)	V_e (m/s)	V_e/V_i	Virtual Cathode?
2.1	1.5	1.0	419386	10.94	Yes
2.2	1.5	0.1	132621	3.46	No
2.3	1.3	8.36E-4	12123	1.0	Yes
2.4	1.3	2.09E-4	6061.5	0.5	Yes

Table 2: Parameters and Result for Simulation Set 2.

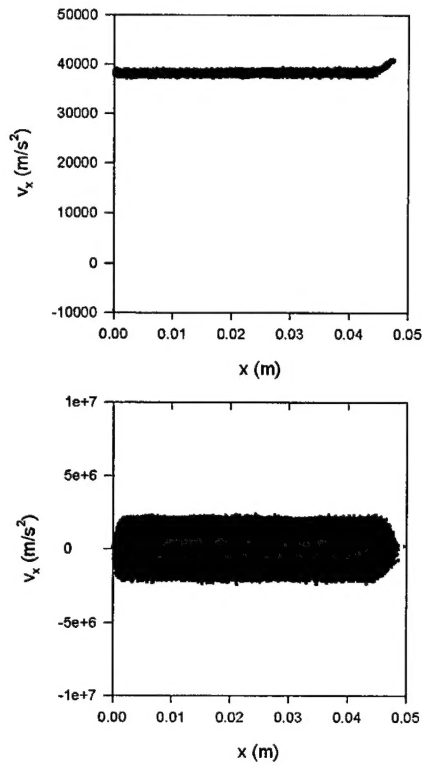


Figure 9: $V_x - x$ phase space for Case 1.5.
 $\tau = 1.2 \text{E-}6 \text{ s}$. Top: ions, Bottom: electrons.

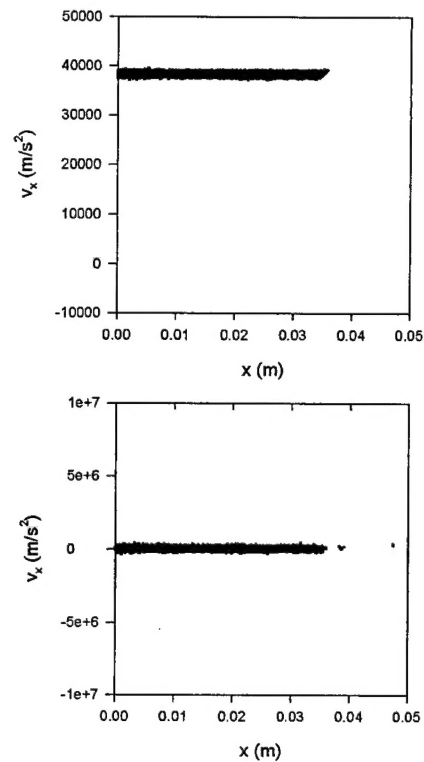


Figure 10: $V_x - x$ phase space for Case 1.6,
 $\tau = 1.2 \text{E-}6 \text{ s}$. Top: ions, Bottom: electrons

emitter surface in the electron phase space plots. Finally, in all simulations one can see the "surfing" effect of the initial ions getting accelerated. This was observed by Buneman and Kooyers¹⁰ as well.

As can be seen in the simulations and is borne out by reality, the system seeks space charge neutralization at the cost of electron momentum. The

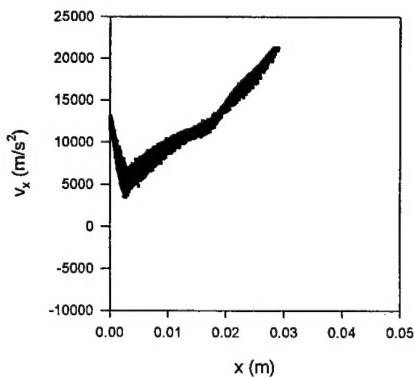


Figure 11: $V_x - x$ phase space of ions for Case 2.3. $\tau = 1.8 \text{E-}6 \text{ s}$

necessity of maintaining a sufficiently small excess of electron velocity in low beam energy cases indicates that it is necessary for low-power neutralization devices to operate in a low-temperature regime, permitting the electrons sufficient interaction time to slow down to ion velocities before exiting the beam.

In all cases a majority of the electrons do get trapped in a potential well created by the ion beam. Due to the greater energy obtained by the electrons in unneutralized cases, the "surfing" acceleration is far more noticeable and may play a part in the instability of the beam, drawing ions further into the negative well in front of the beam and negating the space charge created by the electrons that forced them to return to the main beam.

The role of the perveance P in beam neutralization is still under exploration. While it is well known that a high perveance beam will develop a virtual cathode much sooner than one with a lower perveance, its effect on the ability to allow neutralization has not been fully explored yet. Due to the dramatic variance in susceptibility to electron

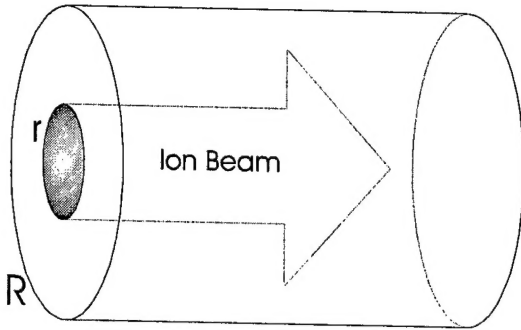


Figure 12: 3-D Simulation Domain

velocity, perveance likely plays a large role in neutralization stability.

3-D Results

The 3-D simulation domain is shown in Figure 12. The cylindrical domain of radius R and length L consists of a circular emission area with radius r where both electrons and ions are injected. While this is unphysical, this was more accurately the case performed in the 2-D simulations. Future work will include a separate neutralizer.

Due to the longer simulation time required of 3-D runs, only a few simulations were performed for the present work. A domain with $L = R = 0.01$ m was generated with an injection surface radius $r = 0.005$ m. The background was held at a density of $1E11$ while the injected density was $1E15$. Injected velocity was set to $10,000$ m/s for the first simulation and increased to $100,000$ m/s for the second. Injected temperatures were held at 0.1 eV for both ions and electrons.

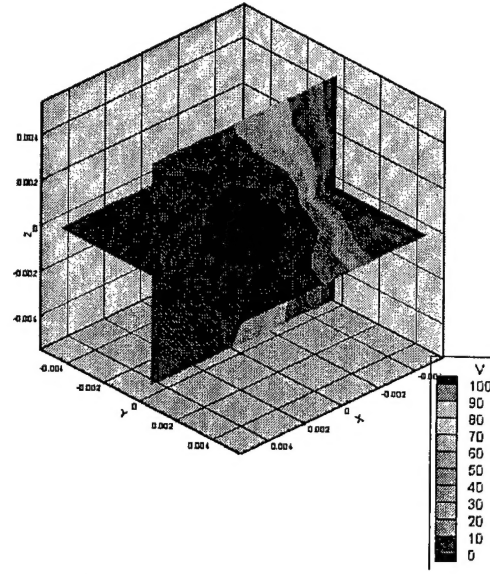


Figure 15: 3-D Potential, $\tau=2.2E-7$ s

As can be seen from Figures 13 and 16, the beam is reflected or neutralized under the same conditions as seen in the 2-D case. Again, we see the formation of the virtual anode reflecting the beam when electron velocities are higher than those of the ions by more than a few factors of two. An interesting result is in Figure 15, where the unneutralized beam "arcs" past the ions before returning and trapping very efficiently in the forward region of the ion beam. This indicates that the electron trapping mechanisms are of significantly different strength in 3-D as compared to 2-D.

We do see the "surfing" effect observed in 2-D here as well. The double hump of the accelerated head corresponds to the beginning of the trapped electrons, which are accelerating the head of the ion

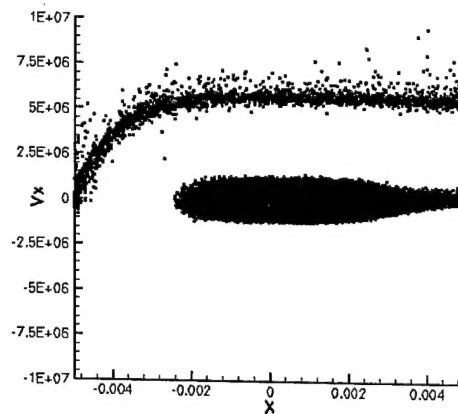


Figure 14: 3-D $V_x - x$ phase space for electrons. $\tau=2.2E-7$ s

beam. In the Figure 14, we see the potential distribution in case 3.1. The virtual cathode is plainly visible. Its location, however, is strange as it corresponds to the trapped electron concentration rather than the location of the slowest ions.

The second run does show a potential well, but the ions have accelerated out of it without the "surfing" seen in the first run indicating a more stable solution. Even though the potential shows large increase across the domain, there does not seem to be the same cathode formation as we have seen in other cases.

CONCLUSIONS

The history of electric propulsion neutralization development was presented along with the outstanding problems therein. Simulations were performed using both 2-D and 3-D PIC codes, demonstrating computationally the neutralization of an ion beam. The process of neutralization was shown to be dependent on the electron to ion velocity ratio. This compares favorably with the observed behavior of electrostatic thrusters and the theories presented in earlier works.

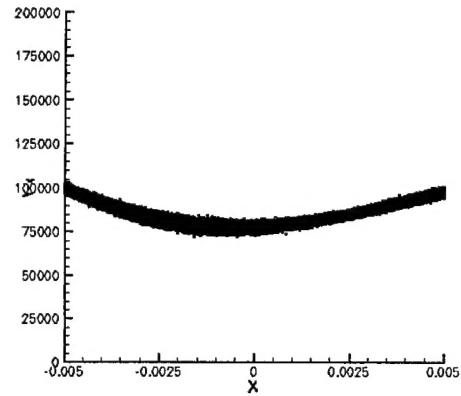


Figure 16: $V_x - x$ Phase Space for Ions in 3-D Case 2. $\tau=2.2E-7$ s

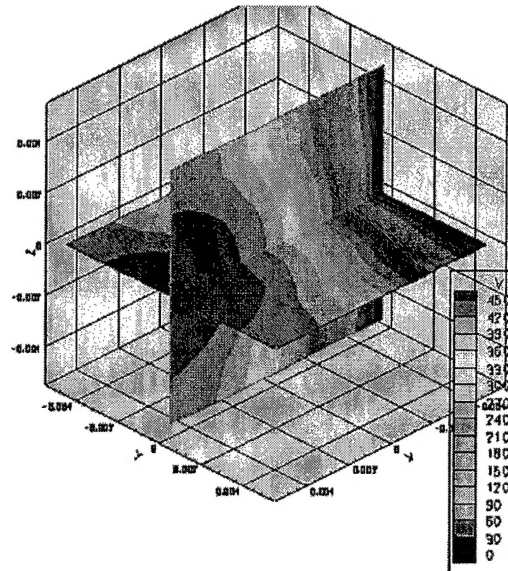


Figure 17: Potential contours for 3-D Case 2. $\tau=2.2E-7$ s

REFERENCES

- ¹ Verboncoeur, J.P., M.V. Alves, V. Vahedi, and C.K. Birdsall, "Simultaneous Potential and Circuit Solution for 1d bounded Plasma Particle Simulation Codes," *J. Comp. Physics*, 104, pp. 321-328, February 1993.
- ² Vahedi, V., C.K. Birdsall, M.A. Lieberman, G. DiPeso, and T.D. Rognlien, "Verification of frequency scaling laws for capacitive radio-frequency discharges using two-dimensional simulations," *Phys. Fluids B* 5 (7), pp. 2719-2729, July 1993.
- ³ V. Vahedi and G. DiPeso, "Simultaneous Potential and Circuit Solution for Two-Dimensional Bounded Plasma Simulation Codes," *J. Comp. Phys.* 131, pp. 149-163, 1997. (Work begun at U.C. Berkeley)
- ⁴ Gatsonis, N.A. and Spirkin, A. "Unstructured 3D PIC Simulations of Field Emission Array Cathodes for Micropropulsion Applications." 38th Joint Propulsion Conference, Indianapolis, IN, July 7-10 2002.
- ⁵ Spirkin, A. and Gatsonis, N.A. Unstructured 3D PIC Simulation of Plasma Flow in a Segmented Microchannel. 36th AIAA Thermophysics Conference, Orlando, FL, June 23-26 2003.
- ⁶ Ramo-Wooldridge Staff. "Electrostatic Propulsion." Proceedings of the IRE, Vol. 48, No. 4, April 1960.
- ⁷ Seitz, R.N. et al. "Present Status of the Beam Neutralization Problem." *Progress in Astronautics and Rocketry Volume 5: Electrostatic Propulsion*, p.383-422, Academic Press, New York, 1961.
- ⁸ Baldwin, G.C. "Neutralization of Ion Beams for Propulsion by Electron Trap Formation." *Progress in Astronautics and Rocketry Volume 5: Electrostatic Propulsion*, p.275-304, Academic Press, New York, 1961.
- ⁹ French, Park. "Circular Beam Neutralization." *Progress in Astronautics and Rocketry Volume 5: Electrostatic Propulsion*, p. 237-250, Academic Press, New York, 1961.
- ¹⁰ Pearlstein, L.D., Rosenbluth, M.N., and Stuart, G.W. "Neutralization of Ion Beams." *Progress in Astronautics and Aeronautics Volume 9: Electric Propulsion Development*, p.379-406, Academic Press, New York, 1963.
- ¹¹ Mirels, H. "On Ion Rocket Neutralization." *Progress in Astronautics and Rocketry Volume 5: Electrostatic Propulsion*, p.373-381, Academic Press, New York, 1961.
- ¹² Buneman, O. and Kooyers, G. "Computer Simulation of the Electron Mixing Mechanism in Ion Propulsion." *AIAA Journal*, Vol. 1, No. 11, p.2525-2528, November 1963.
- ¹³ Wadhwa, R.P. et al. "Two-Dimensional Computer Experiments on Ion-Beam Neutralization." *AIAA Journal*, Vol. 3, No. 6, p.1076-1081, June 1965.
- ¹⁴ Jahn, R.G. *Physics of Electric Propulsion*. McGraw-Hill, New York, 1968.
- ¹⁵ Tajmar, M. and Wang, J. "Three-Dimensional Numerical Simulation of Field-Emission-Electric-Propulsion Neutralization." *Journal of Propulsion and Power*, Vol. 16, No. 3, p.536-544, May 2000.
- ¹⁶ Tajmar, M. and Wang, J. "Three-Dimensional Numerical Simulation of Field-Emission-Electric-Propulsion Backflow Contamination." *Journal of Spacecraft and Rockets*, Vol. 38, No. 1, p.69-78, January 2001.
- ¹⁷ Pawlik, E.V. "Neutralization of a Movable Ion Thruster Exhaust Beam." *JPL Space Programs Summary 37-58*, Vol. III, 1969.
- ¹⁸ Wang, et al. "Three-Dimensional Particle Simulations of Ion Propulsion Plasma Environment Deep Space 1." *Journal of Spacecraft and Rockets*, Vol. 38, No. 3, May 2001.
- ¹⁹ Othmer, C. et al. "Three-dimensional simulations of ion thruster beam neutralization." *Physics of Plasmas*, Vol. 7, No. 12, p.5242-5251, Dec. 2000.
- ²⁰ Othmer, C. et al. "Numerical Simulation of Ion Thruster-Induced Plasma Dynamics - The Model and Initial Results." *Advances in Space Research*, Vol. 29, No. 9, p.1357-1362, Elsevier Science Ltd., UK, 2002.
- ²¹ Rayman, M.D. "The Successful Conclusion of the Deep Space 1 Mission: Important Results Without a Flashy Title." IAC-02-Q.5.2.03, 53rd International Astronautical Congress/World Space Congress, Houston, TX, 10-19 October 2002.
- ²² Brophy, J.R. et al. "Ion Propulsion System (NSTAR) DS1 Technology Validation Report." JPL Publication 00-10, 2000, JPL, Pasadena, CA
- ²³ Wang, et al. "Deep Space One Investigations of Ion Propulsion Plasma Environment." *Journal of Spacecraft and Rockets*, Vol. 37, No. 5, September 2000.
- ²⁴ Häusler, B. et al. "Observations of the Artificially Injected Porcupine Xenon Ion Beam in the Ionosphere." *Journal of Geophysical Research*, Vol. 91, No. A1, p.287-303, January 1986.
- ²⁵ Watson, D. F., "Computing the Delaunay Tessellation with Application to Voronoi Prototypes," *The Computer Journal*, Vol. 24(2), pp. 167-172, 1981.
- ²⁶ Baker, T. J., "Automatic Mesh Generation for Complex Three-Dimensional Regions Using a Constrained Delaunay Triangulation," *Engineering with Computers*, Springer-Verlag, No. 5, pp.161-175, 1989.

²⁷ Birdsall, C.K., A. B. Langdon, "Plasma Physics via Computer Simulations", *Plasma Physics Series*, 1991.

²⁸ Bird, G.A. Molecular Gas Dynamics and the Direct Simulation of Gas Flows, Clarendon Press, Oxford, 1994.

²⁹ Boris, J.P., "Relativistic Plasma Simulation-Optimization of a Hybrid Code", Proceedings of the Fourth Conference on Numerical Simulation of Plasma, Naval Res. Lab, Washington D.C., 3-67, 2-3 November, 1970.